CLM-P815

Bifurcated temperature profiles and the H-mode

C. M. Bishop

UK ATOMIC ENERGY AUTHORITY

Culham Laboratory

CLM-P815

Bifurcated temperature profiles and the H-mode

C. M. Bishop

Culham Laboratory, Abingdon, Oxfordshire, OX14 3DB, UK

(EURATOM/UKAEA Fusion Association)

Abstract

One of the most striking features of the H-mode, in contrast to the L-mode, is the existence of very steep pressure gradients in a narrow layer just inside the plasma boundary. In this paper we show how the existence of H- and L-régimes, together with their characteristic profiles, is a natural consequence of the modified ballooning stability properties near a magnetic separatrix.

(Submitted for publication in NUCLEAR FUSION)

Culham Laboratory
United Kingdom Atomic Energy Authority
Abingdon
Oxfordshire OX14 3DB

1987

I. Introduction

An apparently universal feature of the H-mode in tokamaks is the existence of very steep gradients of temperature and density over a narrow region just inside the plasma boundary [1,2]. The corresponding pressure gradients lie well above the usual (circular tokamak) threshold [3] for the onset of ideal MHD ballooning modes.

Recently, however, it has been shown [4] that close to a magnetic separatrix MHD ballooning stability properties are strongly modified. The most important effect is that whenever the local current density (or equivalently the temperature) exceeds some critical value the first and second regions of ballooning stability coalesce. The plasma is then stable at all values of the pressure gradient. These results are summarised in section II, and may provide a prototype for other curvature driven, shear stabilised modes in the vicinity of a separatrix.

In Section III we use a simple description of transport in the edge region of the plasma to construct those temperature profiles which are everywhere stable to ballooning modes. They fall automatically into two classes. The first class is the usual L-mode in which the whole profile lies in the first stable region. In the second class, which we identify as the H-mode, the edge gradient is in the second region and is connected to the rest of the profile, which is in the first region, above the critical temperature for coalescence. In this way the existence of the H-mode, with its characteristic shape, follows naturally from the modification of the ballooning stability properties due to a magnetic separatrix. Some quantitative comparisons are made between the predicted profiles and experimental results.

The effects of different X-point locations are discussed in Section IV and conclusions are drawn in Section V.

II. Ballooning Stability near a Separatrix.

In Ref. [4] a model equilibrium was used to study the effects of a magnetic separatrix on the stability properties of ideal MHD ballooning

modes. Here we give a brief description of the model and a summary of the stability results. The equilibrium was introduced in Ref. [5] and a detailed account of the methods used to construct it can be found in Ref. [6].

The equilibrium can be regarded as a generalisation of the large aspect ratio s-α model [3] frequently used to describe ballooning stability in circular tokamaks. It is constructed by a local solution of the Grad-Shafranov equation around a single flux surface, and requires a specification of both the shape of the surface and the distribution of poloidal field B_p around the surface. For the s-α model the surface is a circle and B_p is a constant. To model tokamaks with a separatrix we take instead the flux surfaces surrounding a pair of parallel wires. (Note that this straight system is used only to provide the shape of the surface and B_p; the equilibrium itself being calculated in toroidal geometry). The flux surfaces are characterised by a shaping parameter $k \in [0,1]$ with $k = 0$ being a circle (the equilibrium is then precisely the s-α model) and $k = 1$ being a separatrix with the corresponding modulation of B_p around the surface. Example flux surfaces are shown in Fig. 1, which also defines the parameter γ controlling the poloidal location of the x-point.

The equilibrium contains two other parameters, the first of these being the usual pressure gradient parameter α given by

$$\alpha = -\frac{2r}{B_{p0}} \frac{dp}{d\psi} \qquad (1)$$

where p is the pressure, ψ is the poloidal flux, and r and B_{p0} are the values of the minor radius and the poloidal field opposite the X-point. The other parameter is taken to be the current density Λ defined by

$$\Lambda = \frac{rV}{2\pi X_0 B_{p0} \eta} \qquad (2)$$

where X_0 is the major radius, V is the loop volts, and η is the plasma resistivity on the flux surface. This parameter is appropriate for flux surfaces close to a separatrix and replaces the global shear s of circular tokamaks. The ballooning equation corresponding to this equilibrium was solved in Ref. [4] to give the marginally stable α as a function of k, γ and Λ.

In this section and the next we consider $\gamma = 3\pi/4$ which is the X-point configuration corresponding to the PDX tokamak. (The effects of varying γ will be studied in Section IV). In Fig. 2 we plot α against Λ for a flux surface close to the separatrix ($k = 0.95$). At small or negative values of the current density Λ there is a range of unstable pressure gradients separating the first (small α) from the second (large α) stable regions. As Λ is increased the unstable region shrinks, and at a critical value $\Lambda_c \simeq 0.7$ the two regions coalesce. For $\Lambda > \Lambda_c$ all values of the pressure gradient are stable. The dependence on flux surface is shown in Fig. 3 by a plot of α against k for $\Lambda = 0.8$. The unstable region disappears for values of k sufficiently close to 1, i.e. for flux surfaces sufficiently close to the separatrix. Clearly the critical value of Λ will depend on k and a plot of $\Lambda_c(k)$ is given in Fig. 4. This diagram will form the basis of the graphical construction of temperature profiles presented in the next section.

III. Construction of Temperature Profiles.

The stability results described in Section II have important implications for the types of temperature profiles which are stable to MHD ballooning modes. In this section we give a simple graphical construction of such profiles and show that they fall into two classes having many features characteristic of the L-mode and H-mode régimes. These results follow primarily from the topology of the stability diagrams and are largely insensitive to details of the transport processes in the plasma.

To describe the effects of the ballooning mode on transport we adopt the procedure used by Connor, Taylor and Turner [7]. This requires that in the ballooning stable regions the temperature profile is governed by a

simple heat conduction equation, while in the ballooning unstable region the transport coefficient is substantially increased so that the pressure gradient is reduced to the marginally stable value.

We begin by relating the ballooning stability parameters (α, k, Λ) to the temperature profile. To do this we must make some assumptions about the plasma density. We shall follow [7] and take n = constant; although this is not an accurate representation of the density we shall see that the principle qualitative and quantitative results are the same for any reasonable choice for $n(r)$. We choose a specific representation for the density only in order to construct example profiles. (We shall take $n_i = n_e$ and $T_i = T_e$ so that $p = 2n_e T_e$.) The pressure gradient parameter α can now be related to the temperature gradient, and this is done for parameters of the PDX tokamak [2]. Similarly the current density Λ can be related to temperature assuming Spitzer resistivity. Finally the flux surface label k can be related to minor radius using the original straight-wire field configuration [5]:

$$\frac{r}{a} = \frac{\sqrt{1 + k} - 1}{\sqrt{2} - 1} \qquad (3)$$

where a is the radius of the plasma boundary. Fig. 5a shows schematically the ballooning unstable zone in (α, Λ, k) space. There is a corresponding unstable zone in $(dT/dr, T, r)$ space as shown in Fig.5b. We now seek trajectories through this space satisfying the following conditions;

(i) consistency, i.e. $T(r)$ has a derivative which everywhere matches dT/dr,

(ii) $T(r)$ satisfies the background transport equation in the ballooning stable region,

(iii) dT/dr takes the marginally stable value whenever the trajectory enters the unstable zone,

(iv) appropriate boundary conditions are satisfied.

The required profiles may easily be found using a simple graphical construction, as follows. Consider a region close to the edge of the plasma, say $0.8 \leq r/a \leq 1.0$. We now make use of Fig. 4 for $\Lambda_c(k)$. Using the above procedure this corresponds to a graph of critical temperature T_c against r, as shown (for parameters corresponding to the PDX tokamak) in Fig. 6. This graph has the following meaning. If $T < T_c$ there is a range of values of dT/dr which is unstable to ballooning modes. As $T \to T_c$ this range shrinks to zero, and for $T > T_c$ all values of temperature gradient are stable.

The appropriate boundary conditions follow from the fact that the temperature at the separatrix is small, i.e. much less than $T_c(a)$. We therefore take $T(a)=0$. We also know that the bulk of the plasma lies in the first stable region, so we require dT/dr at $r/a = 0.8$ to be at or below the ballooning threshold.

As a specific model of the background transport we follow [7] and choose the thermal conductivity χ to be constant in the ballooning stable regions. Neglecting power deposition and radiative losses in the edge zone the profile in the stable regions will be a straight line whose slope is proportional to the total power P_T deposited in the plasma. Again, a more sophisticated transport model would give somewhat different profiles but would not change the essential results.

We can now construct the required profiles. In Fig. 6 we have also shown the marginally stable values of dT/dr at the separatrix (for $T(a)=0$). There are clearly two classes of profile which can be constructed according to the value of P_T. Low values of P_T give profiles whose edge gradient lie in the first stable region (below curve I in Fig. 6) while at large values the edge gradient lies in the second region (above curve II in Fig. 6). At intermediate values of P_T the edge gradient will by assumption be reduced to the marginally stable value and hence lie along curve I.

Profiles in the first class (edge gradient in the first region) are constrained by the unstable zone to be at or below the ballooning threshold. The profile therefore lies everywhere in the first region, and can be identified with the L-mode.

In the second class the edge gradient lies in the second region. However, we require the profile in the interior of the plasma to be in the first region. The modified stability properties close to the separatrix allow the two parts of the profile to be connected, in a way which is everywhere ballooning stable, at $T \geqslant T_c$. Such a profile is shown by curve B in Fig. 7. The edge gradient is in the second stable region while further into the plasma the profile is held at the marginally stable value. To see why there is a sudden discontinuity of gradient on the T_c curve consider Fig. 8 which shows the trajectory plotted on a graph of dT/dr against T/T_c. Point (i) corresponds to $r/a = 0.8$ and the gradient is limited to the marginal value. As we move closer to the separatrix so T approaches T_c at point (ii). The gradient is then no longer ballooning limited and can jump to the value determined by the background transport at point (iii). Finally the section from points (iii) to (iv) corresponds to the steep edge gradient lying in the second stable region.

This second class of profile automatically has a very steep edge gradient extending a short way into the plasma. We identify these profiles with the H-mode. There exists a minimum P_T required to get an H-mode, this being the value at which the background transport gives a gradient corresponding to curve II in Fig. 6. (The existence of a minimum power threshold for H-mode is well known experimentally). If the power is increased above this value adiabatically the profile will remain in the L-mode, with the edge gradient constrained to the marginal value. However, if the edge temperature can be momentarily raised (e.g. by the passage of a sawtooth heat pulse) then the transition into H-mode can occur. There is a bifurcation of the temperature profiles so that L- and H-mode can both occur at the same value of P_T.

As well as predicting the shape of the profiles this picture of the H-mode is also in quantitative agreement with experimental results. The

temperature T^* at the top of the steep H-mode edge gradient, from Fig.7, is around 350eV in good agreement with PDX data published in Ref.[2]. This prediction for T^* comes from the dimensionless parameter Λ_c and depends only on the assumption of Spitzer resistivity. We can also compare theoretical values of α with data from Ref. [2]. Note that because it is values of α rather than dT/dr which are used this comparison depends only on the stability calculation results and not on any assumptions about density profile, background transport etc. For the L-mode of Ref. [2] $\alpha \simeq 0.35$ in the edge, which from Fig. 3 is clearly in the first stable region. For the H-mode the steep edge gradient gives $\alpha \simeq 3.6$ which is well into the second stable region. Away from the edge $\alpha \simeq 0.52$. Comparison with the coalescence point in Fig. 3 shows that this agrees well with the theoretical value.

IV. Effects of X-point location

So far we have considered a tokamak with a particular X-point location, $\gamma = 135°$. The effects on the stability properties of changing γ are shown in Fig.9 for $90° \leq \gamma \leq 180°$. The first ballooning boundary is essentially independent of γ. This is because the ballooning mode eigenfunction for the first boundary is large only on the outside of the torus (i.e. in the bad curvature region). When the X-point is on the inside of the torus its exact location is unimportant. The second stability boundary, however, shows a strong dependence on X-point location, with the unstable zone shrinking as γ is increased. Note, however, that Λ_c has the opposite dependence and increases slightly with increasing γ.

When the X-point is on the outside of the torus then, as shown in Ref.[4], the ideal interchange mode can be unstable, as well as the ballooning mode. For $\gamma = 0$, which represents the separatrix configuration in JT-60, the interchange mode is dominant, and Fig.10 shows the corresponding $\alpha - \Lambda$ stability diagram for $k = 0.95$. At $\Lambda = 0$ there are again first and second stable regions separated by an unstable region. However, although there is a critical Λ beyond which the mode is completely stable, there also exists a Λ at which the marginally stable

value of α is zero. Any profile which reaches Λ_c must also pass through this point and any pressure gradient there, no matter how small, will drive the mode unstable. This is in marked contrast to the stability properties with the X-point on the inside of the torus, and is reflected by the difficulty of obtaining H-mode operation in JT-60 [8].

V. Conclusions

The presence of a magnetic separatrix has a significant effect on the stability properties of the MHD ballooning mode; in particular a finite current density is able to stabilise the mode completely. We have shown how this effects leads naturally to two classes of ballooning stable profile which we have identified as the L-mode and the H-mode. The predicted H-mode profile has the characteristic steep edge gradient, and a temperature at the top of this gradient which fits well with the experimentally observed values. Pressure gradient values are also in agreement with experiment. The existence of a threshold heating power P_T^{crit} to achieve H-mode arises automatically, as does the existence of both L-mode and H-mode for $P_T > P_T^{crit}$. Finally we have shown that the X-point on the outside of the torus is a special case and leads to interchange instabilties. This is in accord with the difficulties experienced by JT-60 in achieving the H-mode.

I am indebted to R.J. Hastie, S.C. Cowley and J.B.Taylor for numerous valuable discussions. I would also like to thank L.Allen for assistance in plotting Fig.9.

References

[1] F. Wagner et. al. Phys. Rev. Lett. 53 (1984) 1453

[2] S.M. Kaye et. al. J. Nucl. Mater. 121 (1984) 115

[3] J.W. Connor et. al. Phys. Rev. Lett. 40 (1978) 396

[4] C.M. Bishop Nucl. Fusion 26 (1986) 1063

[5] C.M. Bishop et. al. Nucl. Fusion 24 (1984) 1579

[6] C.M. Bishop "Construction of Local Axisymmetric MHD Equilibria" UKAEA, Culham Lab, Abingdon UK, Rep. CLM-R-249 (1985)

[7] J.W. Connor et. al. Nucl. Fusion 24 (1984) 642

[8] JT-60 team, Eleventh International Conference on Plasma Physics and Controlled Nuclear Fusion Research, Kyoto (1986). IAEA-CN-47/A-II-2.

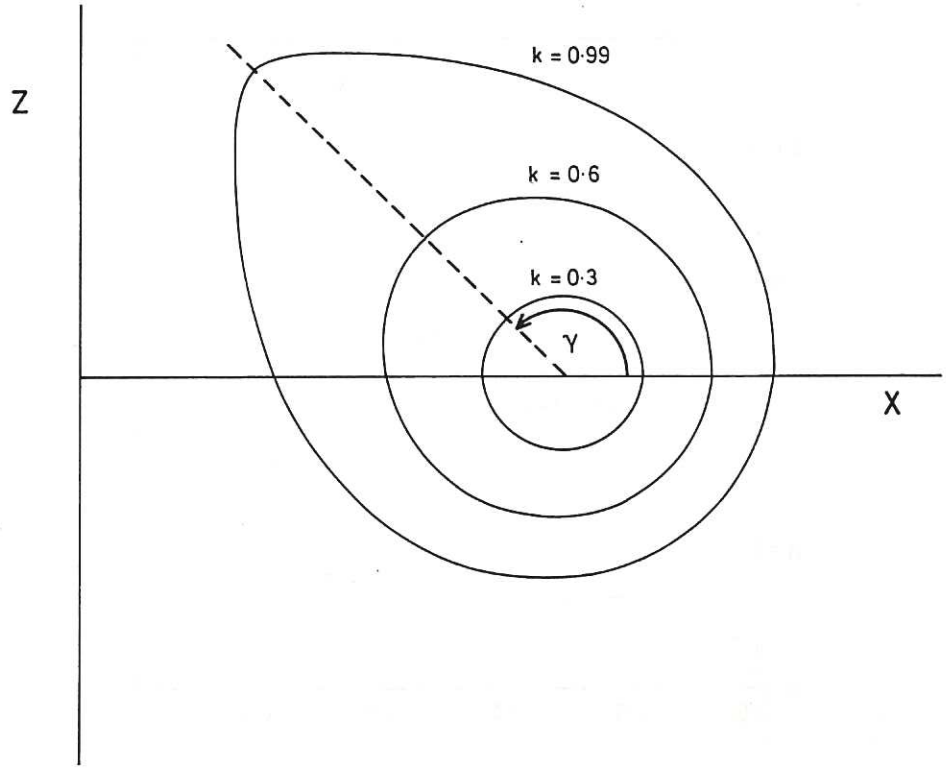

Fig.1 Example of flux surfaces used in the construction of the model equilibrium.

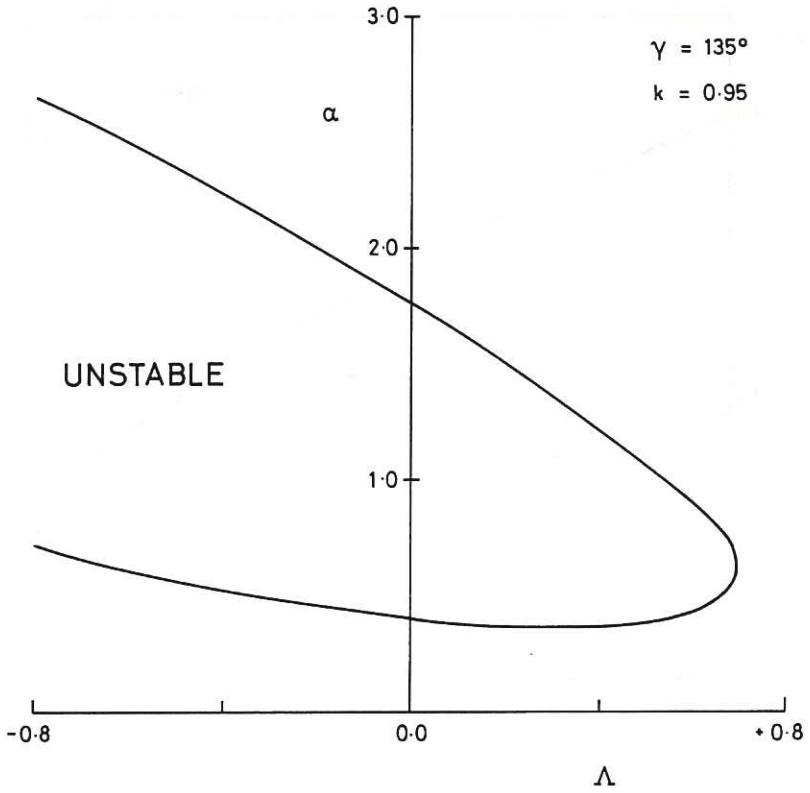

Fig.2 The unstable zone in the $\alpha - \Lambda$ plane showing the existance of a critical value of Λ. ($\gamma = 135°$)

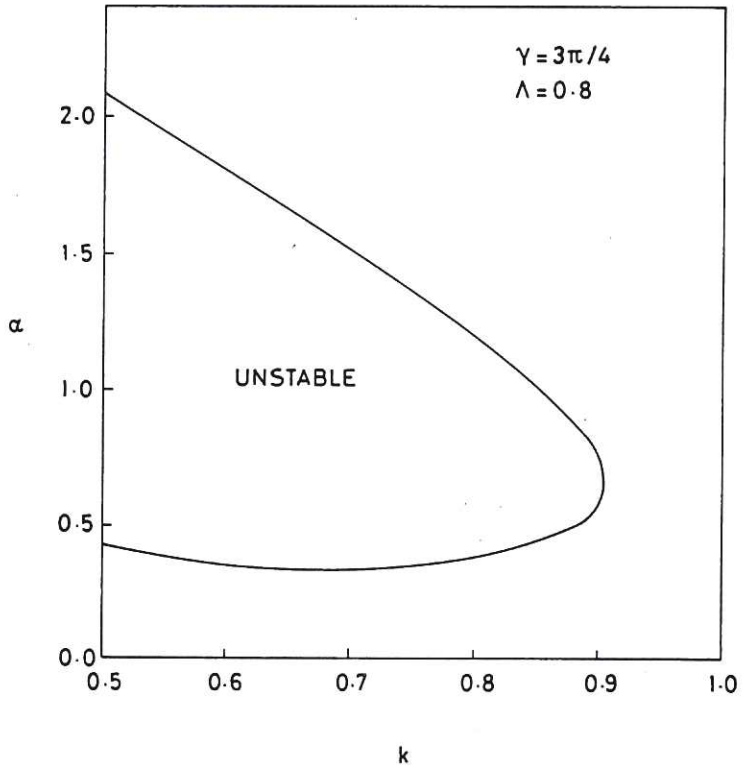

Fig.3 Stability diagram in the $\alpha - k$ plane at $\Lambda = 0.8$ ($\gamma = 135°$)

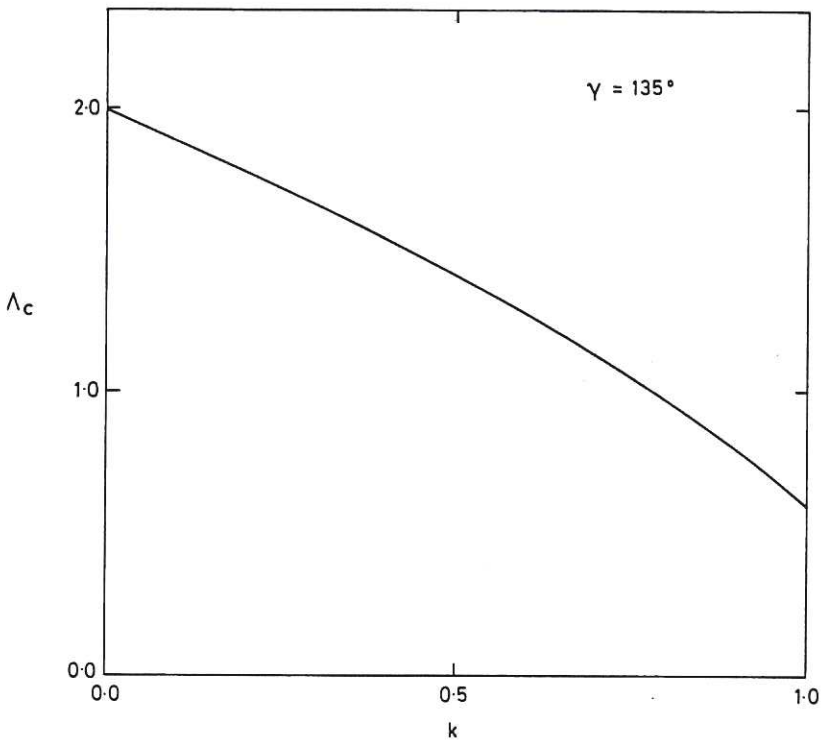

Fig.4 Plot of Λ_c as a function of k ($\gamma = 135°$)

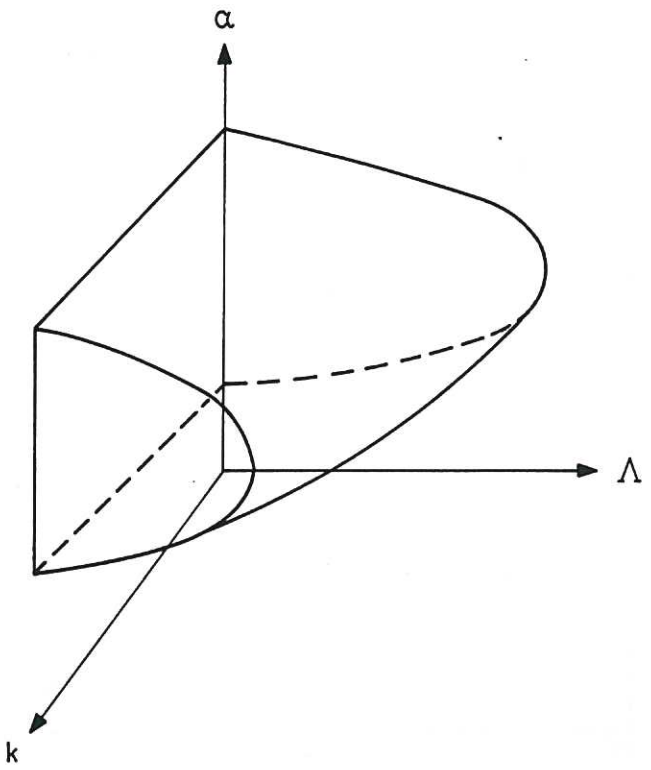

Fig.5a The ballooning unstable zone shown schematically in (α, k, Λ) space.

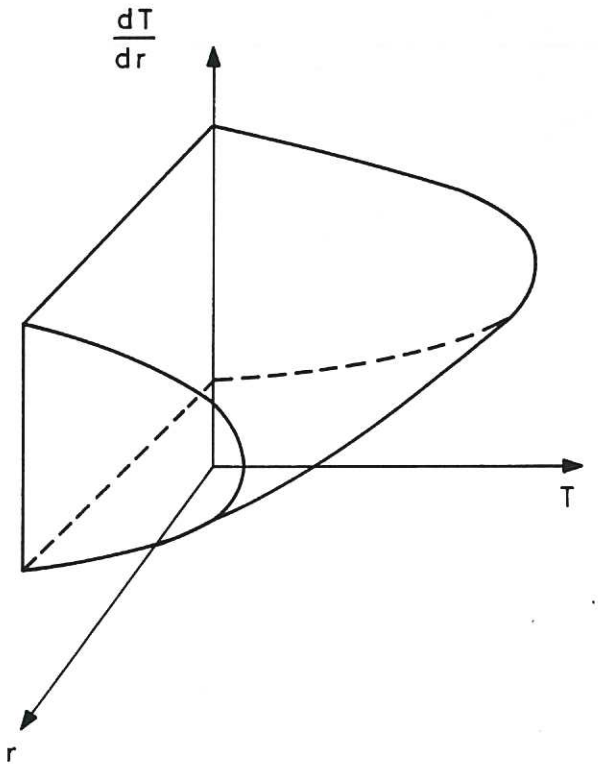

Fig.5b The stability diagram corresponding to Fig.5a but plotted in (T, r, dT/dr) space.

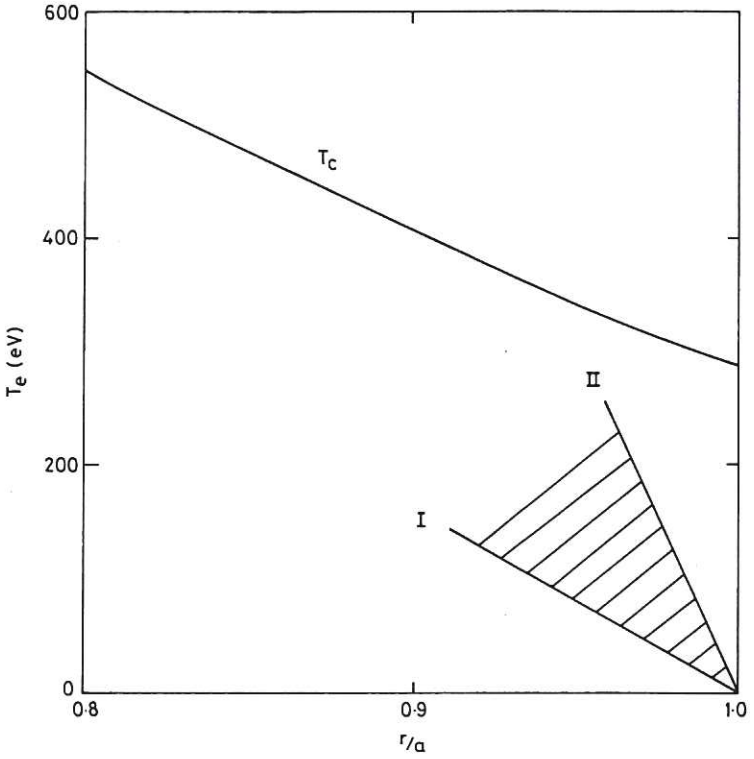

Fig.6 This shows the graph of Fig.4 converted to a $T_c(r)$ curve. Also shown are the first and second marginally stable temperature gradients for r = a , T = 0.

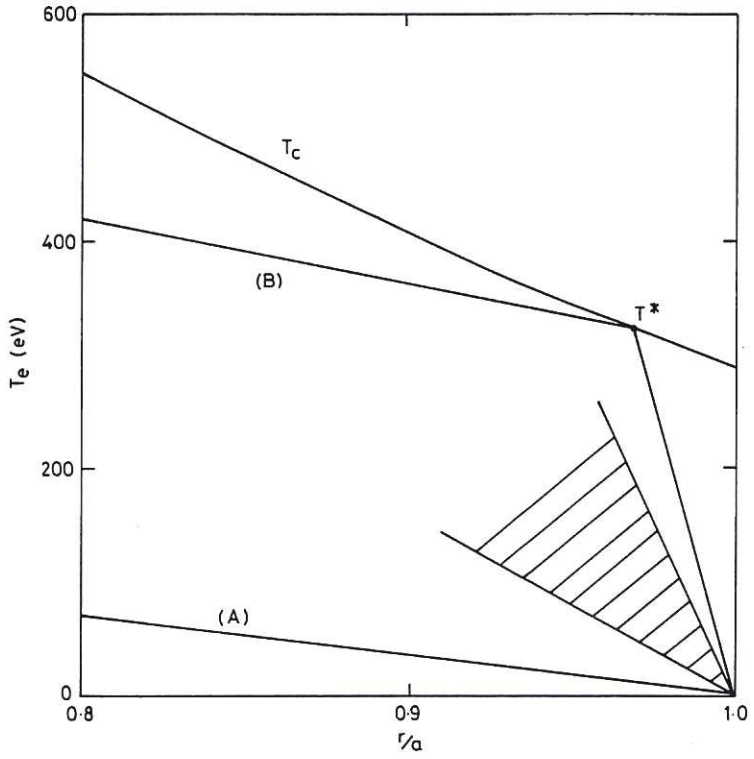

Fig.7 Examples of class I (A) and class II (B) temperature profiles.

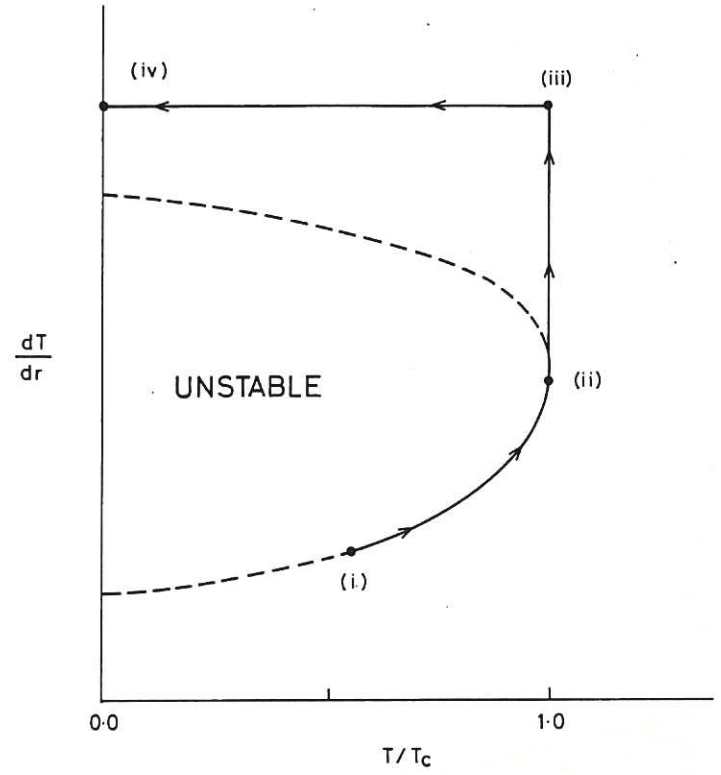

Fig.8 The ballooning unstable zone projected onto the (dT/dr, T/T_c) plane showing the trajectory of a class II profile.

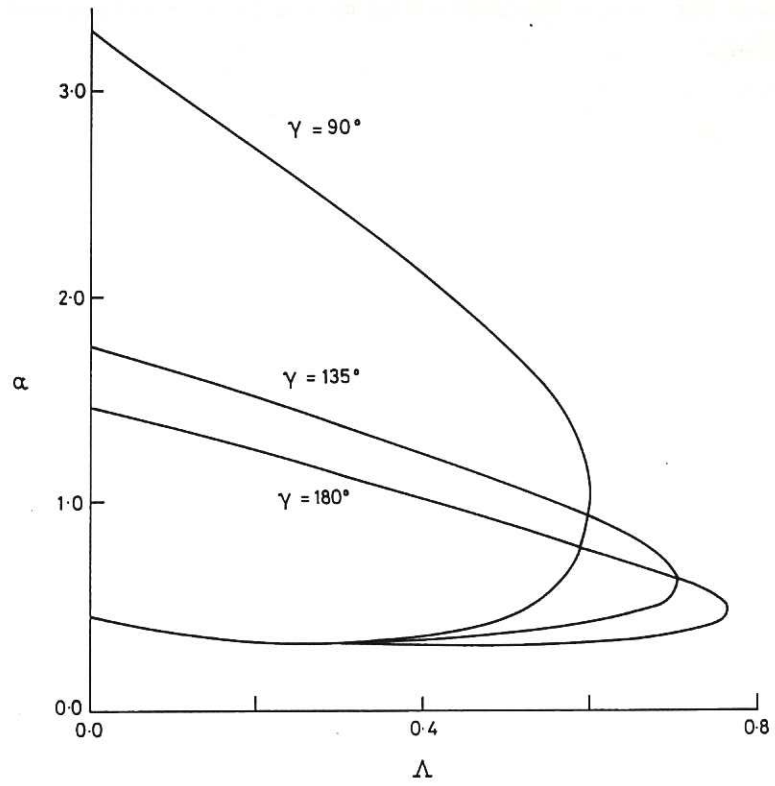

Fig.9 This shows the dependence of the stability boundaries, and Λ_c, on the X-point location γ. ($k = 0.95$)

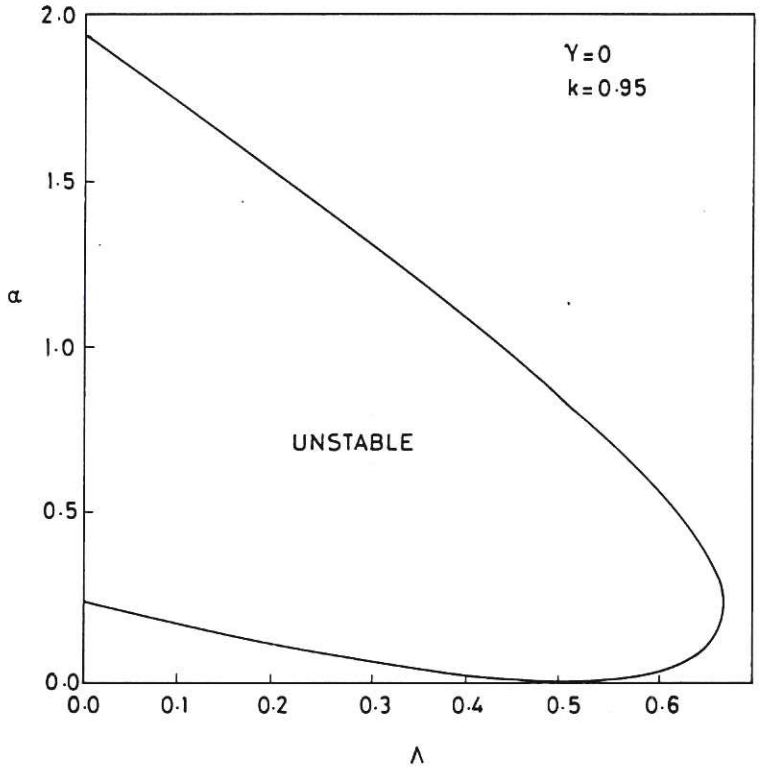

Fig.10 Stability diagram in the $\alpha - \Lambda$ plane of the ideal interchange mode for $\gamma = 0$ corresponding to the X-point configuration in JT-60.